

ORGAN AND EFFECTIVE DOSE COEFFICIENTS FOR CRANIAL AND CAUDAL IRRADIATION GEOMETRIES: PHOTONS

K. G. Veinot^{1,*}, K. F. Eckerman¹ and N. E. Hertel^{1,2}

¹Center for Radiation Protection Knowledge, Oak Ridge National Laboratory, Oak Ridge, TN 37831, USA

²Georgia Institute of Technology, Atlanta, GA 30332-0745, USA

*Corresponding author: veinotkg@y12.doe.gov

Received 1 October 2014; revised 23 February 2015; accepted 8 March 2015

With the introduction of new recommendations of the International Commission on Radiological Protection (ICRP) in Publication 103, the methodology for determining the protection quantity, effective dose, has been modified. The modifications include changes to the defined organs and tissues, the associated tissue weighting factors, radiation weighting factors and the introduction of reference sex-specific computational phantoms. Computations of equivalent doses in organs and tissues are now performed in both the male and female phantoms and the sex-averaged values used to determine the effective dose. Dose coefficients based on the ICRP 103 recommendations were reported in ICRP Publication 116, the revision of ICRP Publication 74 and ICRU Publication 57. The coefficients were determined for the following irradiation geometries: anterior–posterior (AP), posterior–anterior (PA), right and left lateral (RLAT and LLAT), rotational (ROT) and isotropic (ISO). In this work, the methodology of ICRP Publication 116 was used to compute dose coefficients for photon irradiation of the body with parallel beams directed upward from below the feet (caudal) and directed downward from above the head (cranial). These geometries may be encountered in the workplace from personnel standing on contaminated surfaces or volumes and from overhead sources. Calculations of organ and tissue kerma and absorbed doses for caudal and cranial exposures to photons ranging in energy from 10 keV to 10 GeV have been performed using the MCNP6.1 radiation transport code and the adult reference phantoms of ICRP Publication 110. As with calculations reported in ICRP 116, the effects of charged-particle transport are evident when compared with values obtained by using the kerma approximation. At lower energies the effective dose per particle fluence for cranial and caudal exposures is less than AP orientations while above \sim 30 MeV the cranial and caudal values are greater.

INTRODUCTION

International Commission on Radiological Protection (ICRP) Publication 103⁽¹⁾ established a revised method for determining the protection quantities for organs and tissues (equivalent doses) and the effective dose. Changes to the defined organs and tissues, their associated tissue weighting factors, radiation weighting factors and the use of sex-specific phantoms from ICRP 110⁽²⁾ required a recomputation of dose coefficients. The ICRP DOCAL task group reported these dose coefficients in ICRP Publication 116⁽³⁾ which replaces ICRP 74⁽⁴⁾ and the International Commission on Radiation Units and Measurements Report 57⁽⁵⁾. In ICRP 116 coefficients for the standard irradiation geometries (anterior–posterior (AP), posterior–anterior (PA), right and left lateral (RLAT and LLAT), rotational (ROT) and isotropic (ISO)) are provided. The photon absorbed dose coefficients of ICRP 116 were based on tracking of secondary particles whereas those of ICRP 74 used the kerma approximation.

Perhaps the most commonly used orientation in the application of the coefficients in practice is the AP geometry since this corresponds to the standard geometry used for personal dosimeter and instrument calibrations. However, in many operational scenarios these standard geometries may not be appropriate

and angular effects, both on the dosimetric quantities as well as the dosimeter response, must be considered. The irradiation geometries of ICRP-116 also do not account for the possibility of a person being exposed from sources either beneath the feet (caudal) or from overhead (cranial). In operational settings personnel may perform work on contaminated surfaces or with sources positioned overhead. Because the effective dose is dependent upon the doses delivered to organs and tissues, and since these organs and tissues are located throughout the body, the caudal (CAU) and cranial (CRA) geometries may result in significantly different effective doses compared with the six geometries addressed in ICRP-116.

MATERIALS AND METHODS

Protection quantity calculations

As in previous ICRP recommendations, such as ICRP 26⁽⁶⁾ and ICRP 60⁽⁷⁾, the method for determining protection quantities begins with calculating doses to organs and tissues using mathematical phantoms. In ICRP 103 methodology, the organ and tissue absorbed dose coefficients are determined for the male and female reference voxel phantoms separately, the appropriate radiation weighting factor applied, then the

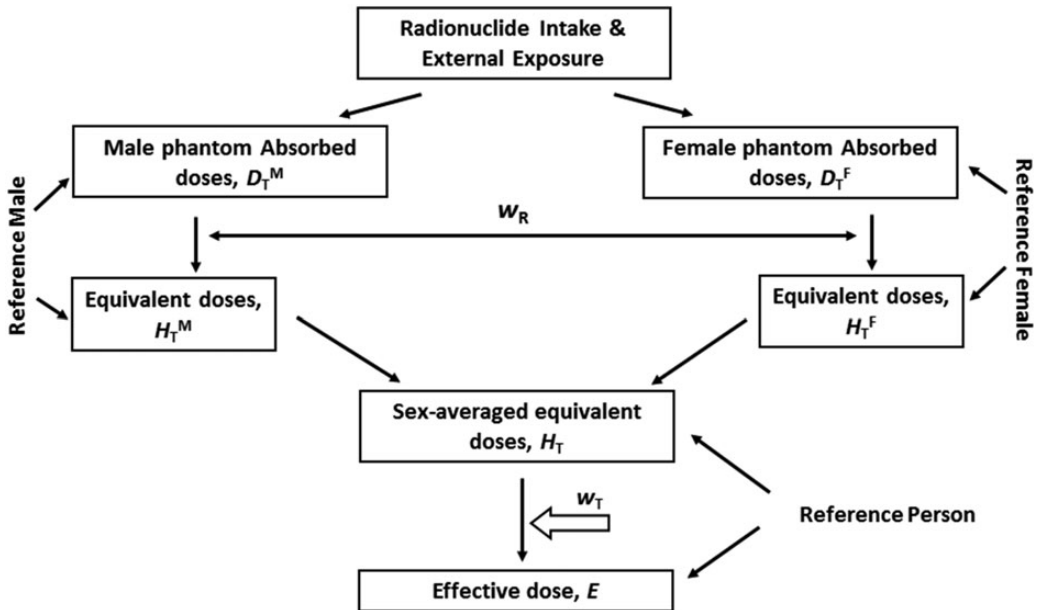


Figure 1. ICRP-103 method for determining equivalent doses and effective dose.

sex-averaged equivalent dose coefficients obtained by averaging the values from the male and female phantoms. The radiation weighting factors, w_R , are given in ICRP-103 for various radiations and energies and for photons ($w_R = 1$). Once the sex-averaged equivalent doses are determined they are weighted by the tissue weighting factors and summed to determine the effective dose coefficient. In the ICRP 103 methodology, the specific organs used to define the remainder are prescribed. For clarity, the procedure for determining the effective dose is shown schematically in Figure 1 and Table 1 lists the tissue weighting factors from ICRP 103.

ICRP Publication 103 defines effective dose, E , as

$$E = \sum_T w_T \left[\frac{H_M^T + H_F^T}{2} \right], \quad (1)$$

where H_M^T is the equivalent dose to organ T of the male phantom, H_F^T is the equivalent dose to organ T of the female phantom and w_T is the organ or tissue weighting factor. The equivalent dose to the organ or tissue is

$$H_T = \sum_R w_R D_{T,R}, \quad (2)$$

where w_R is the radiation weighting factor and $D_{T,R}$ is the absorbed dose to tissue or organ T from incident radiation R .

Table 1. Organ and tissue weighting factors specified in ICRP Publication 103⁽¹⁾.

| Organ or tissue | w_T |
|---|-------|
| Red bone marrow (spongiosa), lung, colon, stomach, breast, remainder ^a | 0.12 |
| Gonads | 0.08 |
| Bladder, esophagus, liver, thyroid | 0.04 |
| Bone surface (endosteum), brain, salivary glands, skin | 0.01 |

^aAdrenals, ET region, gall bladder, heart, kidneys, lymph nodes, muscle, oral mucosa, pancreas, small intestine, spleen, thymus, prostate (male) and uterus (female).

Reference phantoms

The reference phantoms of ICRP 110⁽²⁾ were used for all calculations. These three-dimensional phantoms are volumised-pixel (voxel) representations of male and female subjects based on high-resolution scans. The male phantom contains almost two million voxels with each rectangular solid being $8 \times 2.137 \times 2.137$ mm. The female phantom contains almost four million voxels with each being $4.84 \times 1.775 \times 1.775$ mm. Tissue compositions and densities are based on ICRP 89⁽⁸⁾ information. The male phantom is 1.76 m in height and has a mass of 73 kg while the female is 1.63 m tall and has a mass of 60 kg. Both subjects were scanned while laying prone so the phantoms do display some flattening. Additionally, the female head position slightly favours a head down orientation.

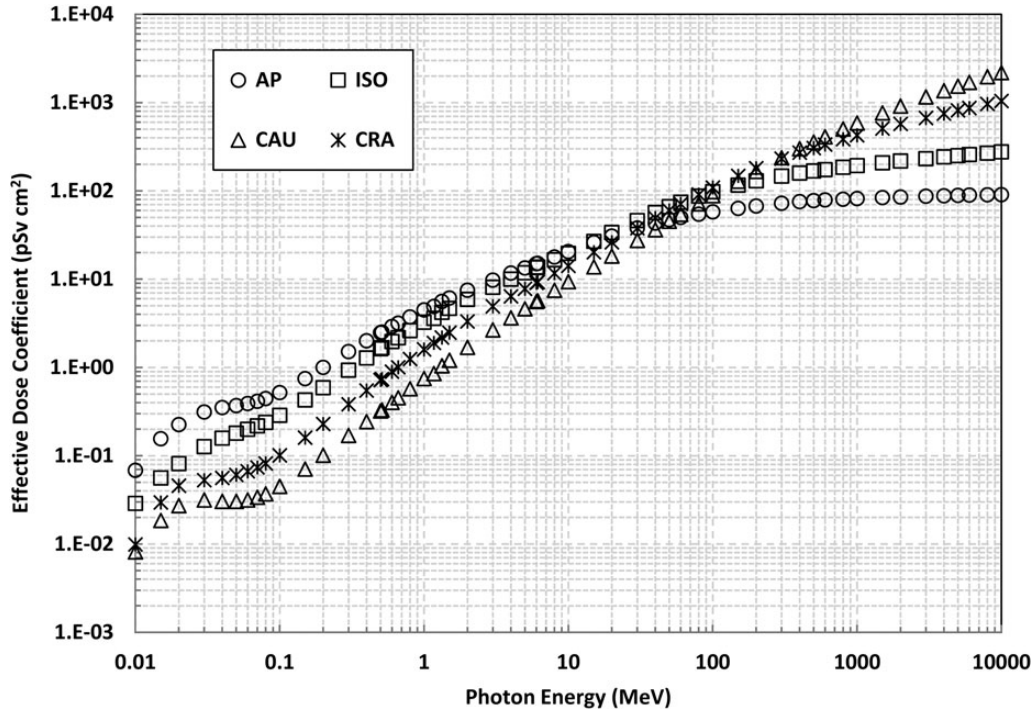


Figure 2. AP, CAU and CRA effective dose coefficients.

Because of the voxel resolution, exact calculations to sensitive regions of the skin (e.g. a depth of 0.07 mm) and to the lens of the eye are not possible, however, for the calculations reported here the dose to those voxels defining the skin were used. Lens of the eye dose coefficients are not reported. Differences in phantom size and organ mass impact the dose coefficients for certain organs because of shielding effects and degree that charged-particle equilibrium is established at longer pathlengths within the body.

Reference radiation field orientations

For caudal and cranial calculations, planar monoenergetic photon sources were oriented either below the feet or over the head with particles directed parallel to the long-axis of the phantom. Source areas were sufficiently large to ensure the entire cross-sectional area of the phantom was within the radiation field.

Calculational method

Calculations were performed using the MCNP6.1⁽⁹⁾ radiation transport code along with ENDF-B VII cross sections. Both the male and female voxel phantoms from ICRP Publication 110 were modelled and irradiated with planar sources oriented upward from below (CAU) or downward from above (CRA) the

phantoms in a vacuum. Organ equivalent doses were computed using both the kerma approximation and tracking the secondary particles. For kerma calculations the energy deposition tally (F6 in MCNP nomenclature), which essentially multiplies the fluence by kerma factors, was employed while absorbed doses were determined using a variant of the pulse-height tally (*F8 tally in MCNP nomenclature). The former tally results in what has traditionally been called the 'kerma approximation' to absorbed dose; while the latter tally provides a more accurate computation of the absorbed dose since it does not assume all energy from interactions is deposited at the interaction site and tracks the secondaries created in the interactions. The dose coefficient energy grid duplicated that used in ICRP Publication 116 and ranged in energy from 10 keV to 10 GeV. The electron and photon lower energy cut-offs were 1 keV. Organ and effective dose coefficients were normalised to particle fluence and are presented in units of pSv cm².

Because of the segmentation of the cortical (bone surface) and spongiosa (red bone marrow) regions these doses were tallied individually and mass weighted to determine the total bone surface and red bone marrow doses. This method is in accordance with that used for ICRP Publication 116.

Tally uncertainties were minimised, although some organs that received small doses had large tally

uncertainties. In cases where these organs and tissues did not significantly contribute to the effective dose this uncertainty was accepted as a practical limitation on computation time. When the organs or tissues were significant contributors to effective dose (the weighted organ equivalent dose, $w_{T}H_{T}$ was greater than 1 % of the effective dose), additional particle histories, in some instances 20 million, were executed to reduce the uncertainty to <3 %. In the cases of the bone surface and the red bone marrow the contributor tally errors were propagated using mass weighting. The effective dose error was determined by propagating the sex-averaged, organ weighted equivalent doses in quadrature.

RESULTS AND DISCUSSION

Effective dose coefficients for cranial (CRA) and caudal (CAU) exposures are shown in Figure 2 along with AP irradiation geometry values from ICRP Publication 116. Ratios of the CAU and CRA effective dose coefficients to AP are shown in Figure 3. Figures 4 and 5 compare the CAU and CRA equivalent dose coefficients for the female brain and male skin, respectively. Tabulated results of effective dose for caudal and cranial geometries are listed in Table 2. Tables for all organs and tissue coefficients are available for download from the Oak Ridge National Laboratory Center for Radiation Protection Knowledge website

(<http://crpk.ornl.gov/resources/>) or can be obtained by contacting the authors. Results for kerma are provided on the CRPK website for interested readers.

The differences between caudal and cranial exposures on organ doses are evident, and not unexpected. The differences in organ doses between the male and female are a consequence of organ location within the body, phantom mass and size and phantom posture itself. While doses to the brain from CAU exposures are smaller at low photon energies, they exceed the AP and CRA values above ~ 200 MeV because charged particle equilibrium (CPE) is established to a greater degree as a result of the longer path-length through the body for these geometries relative to AP and the resultant buildup of the electro-magnetic shower⁽¹⁰⁾. Similar effects are seen for other organs and irradiation geometries such as the gonads (Figure 6) and brain (Figure 4). While CPE is maintained for higher particle energies in organs farther from the source and higher absorbed doses result, organs nearer the source (e.g. the gonads in the case of caudal exposure) exhibit dose coefficients similar in magnitude to AP exposure geometries. This combination results in an increase in the effective dose coefficient above 200 MeV. For large organs distributed throughout the body (red bone marrow, bone endosteum and skin) the geometric and CPE effects are smoothed and the dose coefficients do not depart as radically from standard (e.g. AP, PA, etc.) geometries.

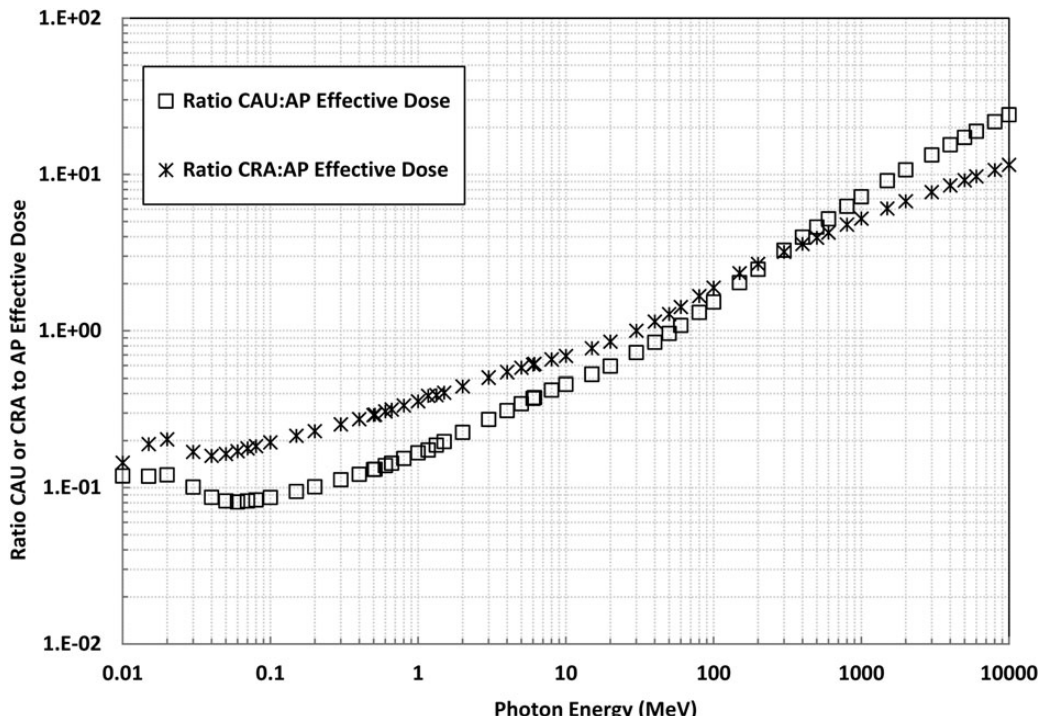


Figure 3. Ratios of CAU and CRA effective dose to AP effective dose coefficients.

CRANIAL-CAUDAL PHOTON DOSE COEFFICIENTS

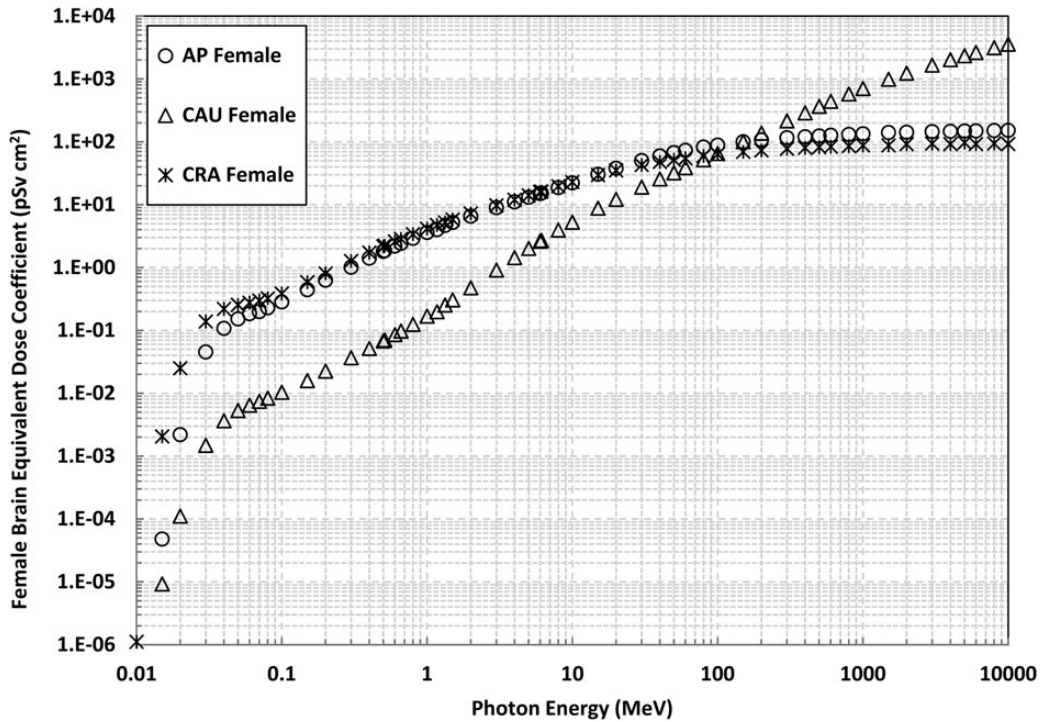


Figure 4. AP, CAU and CRA female brain equivalent dose coefficients.

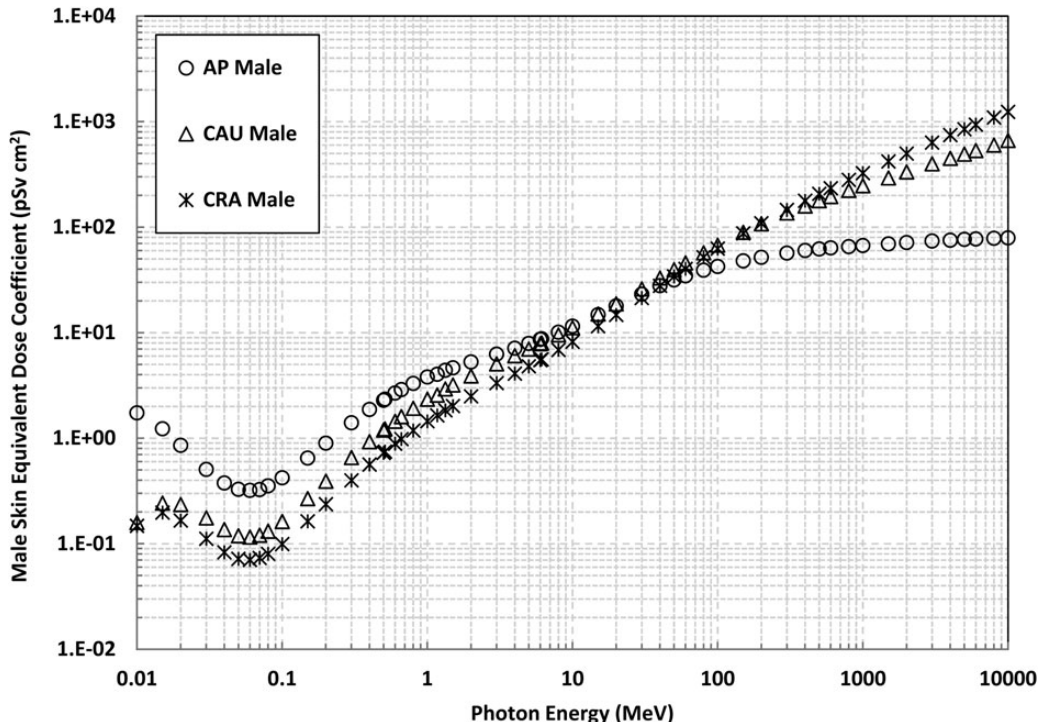


Figure 5. AP, CAU and CRA male skin equivalent dose coefficients.

Table 2. CAU and CRA effective dose coefficients.

| Energy (MeV) | Caudal ($\mu\text{Sv cm}^2$) | Error ($\mu\text{Sv cm}^2$) | Cranial ($\mu\text{Sv cm}^2$) | Error ($\mu\text{Sv cm}^2$) | Energy (MeV) | Caudal ($\mu\text{Sv cm}^2$) | Error ($\mu\text{Sv cm}^2$) | Cranial ($\mu\text{Sv cm}^2$) | Error ($\mu\text{Sv cm}^2$) |
|--------------|-----------------------------------|----------------------------------|------------------------------------|----------------------------------|-----------------|-----------------------------------|----------------------------------|------------------------------------|----------------------------------|
| 0.01 | 8.14E-03 | 2.83E-05 | 9.90E-03 | 3.83E-05 | 6.129 | 5.68E+00 | 1.90E-02 | 9.28E+00 | 2.14E-02 |
| 0.015 | 1.85E-02 | 5.46E-05 | 2.96E-02 | 8.80E-05 | 8 | 7.49E+00 | 1.33E-02 | 1.17E+01 | 1.35E-02 |
| 0.02 | 2.72E-02 | 7.82E-05 | 4.59E-02 | 1.24E-04 | 10 | 9.38E+00 | 1.55E-02 | 1.42E+01 | 1.56E-02 |
| 0.03 | 3.16E-02 | 1.00E-04 | 5.30E-02 | 1.42E-04 | 15 | 1.38E+01 | 6.28E-02 | 2.02E+01 | 6.32E-02 |
| 0.04 | 3.04E-02 | 1.06E-04 | 5.60E-02 | 1.40E-04 | 20 | 1.83E+01 | 7.47E-02 | 2.63E+01 | 7.60E-02 |
| 0.05 | 3.04E-02 | 1.05E-04 | 6.07E-02 | 1.36E-04 | 30 | 2.75E+01 | 8.56E-02 | 3.79E+01 | 9.87E-02 |
| 0.06 | 3.16E-02 | 1.06E-04 | 6.67E-02 | 1.36E-04 | 40 | 3.64E+01 | 1.01E-01 | 4.93E+01 | 1.21E-01 |
| 0.07 | 3.40E-02 | 1.08E-04 | 7.37E-02 | 1.37E-04 | 50 | 4.52E+01 | 1.14E-01 | 6.03E+01 | 1.37E-01 |
| 0.08 | 3.71E-02 | 1.12E-04 | 8.19E-02 | 1.43E-04 | 60 | 5.42E+01 | 1.29E-01 | 7.11E+01 | 1.55E-01 |
| 0.1 | 4.49E-02 | 1.24E-04 | 1.01E-01 | 1.61E-04 | 80 | 7.14E+01 | 1.51E-01 | 9.09E+01 | 1.89E-01 |
| 0.15 | 7.07E-02 | 1.78E-04 | 1.61E-01 | 2.44E-04 | 100 | 8.82E+01 | 1.68E-01 | 1.09E+02 | 2.12E-01 |
| 0.2 | 1.01E-01 | 2.57E-04 | 2.30E-01 | 3.45E-04 | 150 | 1.28E+02 | 2.95E-01 | 1.48E+02 | 2.67E-01 |
| 0.3 | 1.70E-01 | 4.40E-04 | 3.83E-01 | 5.89E-04 | 200 | 1.66E+02 | 3.59E-01 | 1.80E+02 | 3.24E-01 |
| 0.4 | 2.43E-01 | 6.40E-04 | 5.48E-01 | 8.42E-04 | 300 | 2.37E+02 | 4.61E-01 | 2.31E+02 | 5.19E-01 |
| 0.5 | 3.22E-01 | 8.58E-04 | 7.20E-01 | 1.11E-03 | 400 | 3.00E+02 | 5.72E-01 | 2.72E+02 | 5.90E-01 |
| 0.511 | 3.31E-01 | 8.86E-04 | 7.39E-01 | 1.13E-03 | 500 | 3.57E+02 | 7.35E-01 | 3.05E+02 | 6.61E-01 |
| 0.6 | 4.03E-01 | 1.08E-03 | 8.95E-01 | 1.37E-03 | 600 | 4.10E+02 | 8.14E-01 | 3.35E+02 | 7.40E-01 |
| 0.662 | 4.55E-01 | 1.22E-03 | 1.00E+00 | 1.54E-03 | 800 | 5.04E+02 | 9.83E-01 | 3.85E+02 | 8.61E-01 |
| 0.8 | 5.73E-01 | 1.53E-03 | 1.25E+00 | 1.90E-03 | 1000 | 5.88E+02 | 1.14E+00 | 4.27E+02 | 9.73E-01 |
| 1 | 7.49E-01 | 1.98E-03 | 1.60E+00 | 2.39E-03 | 1500 | 7.65E+02 | 1.49E+00 | 5.08E+02 | 1.20E+00 |
| 1.17 | 8.53E-01 | 3.23E-03 | 1.90E+00 | 8.45E-03 | 2000 | 9.12E+02 | 1.63E+00 | 5.74E+02 | 1.05E+00 |
| 1.33 | 1.05E+00 | 3.91E-03 | 2.18E+00 | 4.94E-03 | 3000 | 1.16E+03 | 2.26E+00 | 6.70E+02 | 2.07E+00 |
| 1.5 | 1.21E+00 | 3.09E-03 | 2.48E+00 | 3.60E-03 | 4000 | 1.36E+03 | 2.48E+00 | 7.50E+02 | 2.31E+00 |
| 2 | 1.69E+00 | 4.15E-03 | 3.32E+00 | 4.73E-03 | 5000 | 1.54E+03 | 3.34E+00 | 8.17E+02 | 2.66E+00 |
| 3 | 2.66E+00 | 6.09E-03 | 4.92E+00 | 6.73E-03 | 6000 | 1.69E+03 | 3.55E+00 | 8.70E+02 | 3.47E+00 |
| 4 | 3.64E+00 | 7.82E-03 | 6.39E+00 | 8.40E-03 | 8000 | 1.96E+03 | 4.16E+00 | 9.64E+02 | 3.35E+00 |
| 5 | 4.61E+00 | 9.37E-03 | 7.78E+00 | 9.91E-03 | 10 000 | 2.19E+03 | 4.52E+00 | 1.04E+03 | 4.30E+00 |
| 6 | 5.59E+00 | 1.08E-02 | 9.11E+00 | 1.12E-02 | | | | | |

CRANIAL-CAUDAL PHOTON DOSE COEFFICIENTS

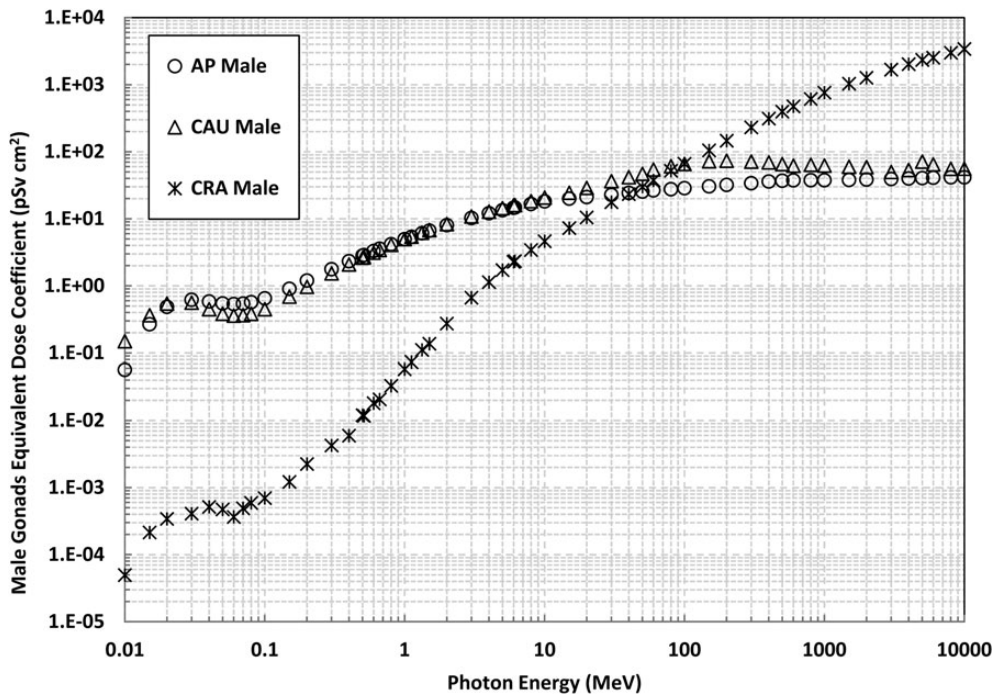


Figure 6. AP, CRA and CAU equivalent dose coefficients for the male gonads.

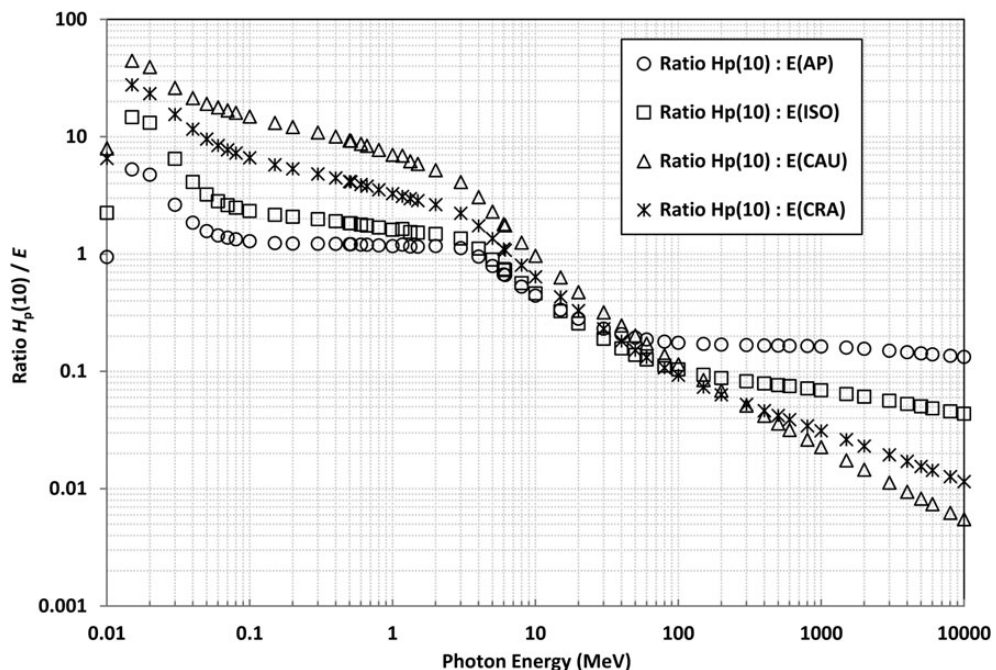


Figure 7. Ratio of $H_p(10)$ to AP, ISO, CRA and CAU effective dose. Values for $H_p(10)$ were taken from Veinot and Hertel⁽¹¹⁾.

The ratios of personal dose equivalent, $H_p(10)$, to the effective dose for AP, ISO, CRA and CAU orientations are shown in Figure 7. The $H_p(10)$ values for Figure 7 were taken from Veinot and Hertel⁽¹¹⁾ and were calculated using full transport of secondary particles. As discussed in Veinot and Hertel⁽¹¹⁾, $H_p(10)$ provides a conservative approximation of the protection quantity up to ~ 3 MeV. For caudal and cranial geometries $H_p(10)$ remains conservative to higher energies (about 6 MeV for cranial and about 10 MeV for caudal). These values do not include response effects of personnel dosimeters.

CONCLUSION

Dose coefficients for caudal and cranial irradiation geometries have been calculated in accordance with ICRP Publication 103. The coefficients differ significantly from AP values for both organ and tissues of ICRP Publication 116, as would be expected. For workers irradiated in these geometries, organ and effective doses can differ significantly from AP values. For the photon energies encountered at most nuclear facilities (i.e. 100 keV to a few MeV) the AP effective dose overestimates the caudal and cranial values by about a factor of 10. Above about 30 MeV the CRA and CAU effective dose is underestimated by AP values.

REFERENCES

1. International Commission on Radiological Protection (ICRP). *The 2007 Recommendations of the International Commission on Radiological Protection*. ICRP Publication 103. Ann. ICRP **37** (2–4). Elsevier (2007).
2. International Commission on Radiological Protection (ICRP). *Adult Reference Computational Phantoms*. ICRP Publication 110. Ann. ICRP **39** (2). Elsevier (2009).
3. International Commission on Radiological Protection (ICRP). *Conversion Coefficients for Radiological Protection Quantities for External Radiation Exposures*. ICRP Publication 116. Ann. ICRP **40** (2–5). Elsevier (2010).
4. International Commission on Radiological Protection (ICRP). *Conversion Coefficients for Use in Radiological Protection Against External Radiation*. ICRP Publication 74. Ann. ICRP **26** (3–4). Pergamon Press (1996).
5. International Commission on Radiation Units and Measurements (ICRU). *Conversion Coefficients For Use In Radiological Protection Against External Radiation*. ICRU Report 57. ICRU (1998).
6. International Commission on Radiological Protection (ICRP). *Recommendations of the International Commission on Radiological Protection*. ICRP Publication 26. Ann. ICRP **1** (3). Pergamon Press (1977).
7. International Commission on Radiological Protection (ICRP). *1990 Recommendations of the International Commission on Radiological Protection*. ICRP Publication 60. Ann. ICRP **21** (1–3). Pergamon Press (1991).
8. International Commission on Radiological Protection (ICRP). *Basic Anatomical and Physiological Data for Use in Radiological Protection Reference Values*. ICRP Publication 89. Ann. ICRP **32** (3–4). Pergamon Press (2002).
9. Pelowitz, D. B. (ed.) *MCNP6 User's Manual Version 1.0*. LA-CP-13-00634 Rev. 0. Los Alamos National Laboratory (2013).
10. Rogers, D. W. O. *Fluence to dose equivalent conversion factors calculated with EGS3 for electrons from 100 keV to 20 GeV and photons from 11 keV to 10 GeV*. HPJ **46**(4), 891–914 (1984).
11. Veinot, K. G. and Hertel, N. E. *Personal dose equivalent conversion coefficients for photons to 1 GeV*. Radiat. Prot. Dosim. **145**(1), 28–35 (2010).